J. Water Environ. Nanotechnol., 5(3): 234-245 Summer 2020

ORIGINAL RESEARCH PAPER

Investigation on Polysulfone Blended NH_2-MIL125 (Ti) Membrane for Photocatalytic Degradation of Methylene Blue dye

Abbas Ahmadi [1,2], Mohammad-Hossein Sarrafzadeh[1*], Maryam Mohamadi[1], Zeinab Mahdigholian[1], Akram Hosseinian[2]

[1] *UNESCO Chair on Water Reuse (UCWR), School of Chemical Engineering, College of Engineering, University of Tehran, Tehran, Iran*
[2] *Department of Engineering Science, College of Engineering, University of Tehran, Tehran, Iran*

Received: 2020-05-2 Accepted: 2020-06-30 Published: 2020-08-01

ABSTRACT
Membrane hybrid processes represent innovative separation technologies in which each technique complements the advantages and overcomes the challenges of the other. Dye removal from wastewater is an application in which membrane hybrid processes are widely applied. The focus of this study is also on the development of a membrane hybrid process for dye removal from wastewater. Different proportions of NH_2-MIL125(Ti) were embedded in a PSf polymeric membrane through the phase inversion method. The membrane performance was evaluated for the degradation of a Methylene Blue dye under three different light conditions of dark environment, UV, and visible light irradiation. The synthesized membranes were characterized by FTIR, XRD, and FE-SEM measurements. NH_2-MIL125(Ti) nanoparticles were successfully entrapped in the PSf membrane through a simple phase inversion method and the addition of NH_2-MIL125(Ti) to the PSf membrane resulted in the improvement of membrane porosity. Up to 60% of dye degradation was observed with the 1% NH_2-MIL125(Ti)/PSf nanocomposite membrane after 300 minutes of UV light irradiation. Degradation kinetics followed a pseudo-first-order model, indicating possible changes in the membrane properties upon irradiation with simulated solar radiation.

Keywords: *Dye removal; Membrane; MOF; Polysulfone; Photocatalyst*

How to cite this article
Ahmadi A., Sarrafzadeh MH., Mohamadi M., Mahdigholian Z., Hosseinian A. Investigation on Polysulfone Blended NH_2-MIL125 (Ti) Membrane for Photocatalytic Degradation of Methylene Blue dye. J. Water Environ. Nanotechnol., 2020; 5(3): 234-245.
DOI: 10.22090/jwent.2020.03.004

INTRODUCTION

Human demand, consumption, and industrialization increased dye requirement in many industries such as paper, plastic, food, textile, tannery, cosmetics, etc. China, India, and the USA have the highest export rate of textiles around the world [1], [2]. Different types of reactive dyes are highly toxic even in minor concentrations (often less than 1 mg/l) and may cause serious problems for human health and aquatic life due to changing the level of Biological Oxygen Demand (BOD) in water [3], [4]. This issue encouraged the governments in most countries to enact laws and instructions that prevent the discharge of dye-containing wastewaters into the environment without proper treatments [5], [6].

Methylene Blue ($C_{16}H_{18}N_3ClS$) is categorized as a cationic dye. MB is widely utilized in textile industries, and its complex structure provides high resistance under intense light and heat irradiation [7]. Wastewaters containing MB, that are being discharged into the environment, typically include the MB concentration range of 10-200 ppm that causes severe damage to the environment and humans health [8] and could release aromatic

* Corresponding Author Email: *sarrafzdh@ut.ac.ir*

amines such as benzedrine and bethylene, which are carcinogenic and could cause diseases such as gastrointestinal problems, anemia, and profuse sweating [9].

Although numerous methods of dye removal such as chemical, biological and physical techniques have been studied, there is still a gap for high-performance methods which are capable of dye removal from wastewater with high efficiency [10]. Membrane separation is an effective and useful approach due to its low costs, potentials for material recovery, being ecologically friendly, and the removal of various components in a selective manner. However, this technique represents a simple separation function by only transferring pollutants from one phase to another [11], [12]. In recent years, attentions have been attracted to the modified photocatalytic membranes [13]. Photocatalytic reactions could completely degrade organic pollutants. The advantages such as separation and reusability of photocatalysts with low cost and energy, antifouling properties, and fine permeate flux, have made it an efficient method among conventional methods [14], [15]. A combination of membrane separation and the photocatalytic process could be a solution in order to enhance membrane permeability and organic degradation in wastewaters containing hardly-decomposable compounds such as dyes [16]. Several reports have been made in describing the performance of photocatalytic membrane technology for wastewater treatment. For instance, Zioui et al. used photocatalytic modified poly (vinylidene fluoride–trifluoro ethylene) membrane for oily wastewater treatment [17]. It was figured out that the proposed nanocomposite membrane was effective in oil degradation under sunlight irradiation. Kuvarega et al. studied the impacts of enhanced porosity and hydrophilicity on the removal efficiencies of eosin yellow 97% after 4 hours of visible light irradiation [18]. In another study, modifications on the microstructure of photocatalytic membrane by incorporation of N-doped anatase/rutile mixed-phase TiO_2 nanorods improved photocatalytic activity in the degradation of phenol in aqueous solution under UV and visible light irradiation [19].

The photocatalytic process mainly consists of semiconductor catalysts such as ZnO, TiO_2, etc. The recombination of electron-hole and induced electron with sufficient energetic photons(which are received from UV or visible light sources), affects the dye degradation rate. The properties and structure of photocatalysts such as band-gap energy(which is the most important factor), particle size distribution, crystal composition, porosity, and surface area, considerably influence the photocatalytic efficiency [20]. The most widely used photocatalyst in photocatalytic membrane reactor (PMR) systems is TiO_2, due to its distinctive characteristics such as nontoxicity, desirable chemical stability and activity, and low price [21].

Metal-organic frameworks (MOFs) are a class of materials in which metal ions/clusters interact with each other through organic bonds to form porous structures. They have the potential to be used in various applications, especially in photocatalysis, which is the main interest of the current research [22]. The NH_2-MIL125(Ti) is a MOF form with cyclic $Ti_8O_8(OH)_4$ oxoclusters and 2-aminoterephthalate ligands and has shown a great affinity to adsorption inbound visible light in the electromagnetic spectrum due to its amino-functionalized structure [23].

The PSf membrane has been widely used as a commercial membrane because of its advantages such as high glass-transition temperature (Tg), high pH tolerance, low price, and noticeable permeability. However, this membrane has some disadvantages due to its inherent hydrophobic nature and membrane fouling which results in flux decline and increasing demand for filtration energy [24], [25]. UV irradiation, blending with hydrophilic nanoparticles, graft polymerization, and spin coating are examples of the solutions that have been suggested, in order to overcome the inherent hydrophobicity of polysulfone membrane [18]. Among all these solutions, the blending of TiO_2 with PSf membrane has led to a significantly positive impact on the surface hydrophilicity and promoted the permeate flux [26], [27]. MOF usage in the polysulfone matrix, while facilitating its separation from the degraded pollutant solution, helps to use it in future studies such as in a photocatalytic membrane reactor system. This research focuses on NH_2-MIL125(Ti)/PSf membrane preparation which is employed subsequently for the degradation of MB dye in wastewater. The NH_2-MIL125(Ti)/PSf nanocomposite was characterized by FTIR, XRD, and FESEM. Finally, the nanocomposite's performance for MB removal from synthetic wastewater was studied, under visible light, UV light irradiation, and in a dark environment.

Table 1. Composition of synthesized membrane

Composite membrane	Amount of Nano (g)	MOF/PSf percentage %
PSf	0	0
PSfM 0.2	0.038	0.2
PSfM 0.5	0.095	0.5
PSfM 1	0.19	1

MATERIALS AND METHODS

Methanol (CH_3OH, CAS No. 67-56-1), Dimethylformamide (DMF) (C_3H_7NO, CAS No. 68-12-2), N-Methyl-2-Pyrrolidone (NMP) (C_5H_9NO, CAS No. 872-50-4), and Polyethylene glycol 400 ($C_{2n}H_{4n+2}O_{n+1,}$ CAS NO. 25322-68-3) were supplied by Merck, Germany. Titanium isopropoxide ($C_{12}H_{28}O_4Ti$, CAS No. 546-68-9) was obtained from Alfa Aesar, 2-aminoterephthalic acid ($C_8H_7NO_4$, CAS No. 10312-55-7) was supplied by Sigma Aldrich, and polysulfone ($C_{81}H_{66}O_{12}S_3X_2$, CAS No. 25135-51-7) was provided by BASF. Methylene Blue (MB) ($C_{16}H_{18}ClN_3S$) was used as a model compound. It was supplied by Sigma Aldrich. The dye solution was prepared using distilled water.

Characterization of the NH_2-MIL125(Ti)/PSf nanocomposite

Fourier transform infrared (FTIR) spectroscopy was performed via a Varian 670 FTIR spectrometer recorded at the resolution between 400 and 4000 cm^{-1}. The sample crystallinity was determined by using X-ray diffractometer (XRD) Philips PW 1730 radiation of wavelength 1.540598 A at 40 kV and 30 mA. The diffracted intensity was measured by scanning range of $2\theta = 5 - 80^o$ with a step speed of $3^o.min^{-1}$. Field-emission scanning electron microscopy (FE-SEM) FEI NOVA NanoSEM 450 equipped with an energy dispersive X-ray spectrum (EDS) was used to investigate the surface morphology of the NH_2-MIL125(Ti) and NH_2-MIL125(Ti)/PSf membrane.

EXPERMINTAL

Preparation of NH_2-MIL125(Ti)

The synthesis of the MOF nanoparticles was performed according to the proposed method by Nasalevich et al. as following [28]. First, the mixture of 40 mL dimethylformamide and 10 mL methanol was stirred at room temperature while adding 2.86 g of 2-aminoterephthalic acid to the mixture. After homogenization, 2.86 g of titanium isopropoxide was added slowly (to prevent aggregation) and the mixture was stirred, for a few hours. Afterward, the mixture was placed in a Teflon liner inserted in a stainless steel autoclave reactor and the mixture was heated at 110 °C in an oven for 72 hours. Subsequently, after being cooled in room temperature, the resulting mixture was filtered and washed with a sufficient amount of dimethylformamide (50 mL of DMF per 1 g of product) in order to remove residual linker for 48 hours. Later on, the same procedure was repeated twice using methanol instead of DMF in order to exchange the DMF within the pores. Finally, the resulting solid was dried in dry air with a temperature of 100°C [28].

Preparation of NH_2-MIL125(Ti)/PSf

First, a specific amount of N-Methyl-2-pyrrolidone (NMP) was stirred for 30 minutes and then placed in an ultrasonic bath for further homogenization for another 30 minutes. Afterward, the mixture was stirred again while 19 g of PSf polymers were added gradually. In this regard, the polyethylene glycol (PEG) 400 was used in order to increase the porosity/permeability in the membrane structure, and 4.5 mL of it was added to the solution for membrane fabrication. In order to prevent the generation of bubbles in the polymer solution, the container of the polymer solution was placed in water at 80 ° C for 24 hours. NH_2-MIL125(Ti)/PSf membrane with compositions of 0, 0.2, 0.5 and 1 wt. % were denoted as PSf, PSfM0.2, PSfM0.5, and PSfM1 respectively regarding the amount of MOF which is shown in Table 1.

After preparing the solution, the phase inversion process was carried out to fabricate a membrane with a specific thickness [29]. Subsequently, the casting solution was cast onto flat glass plates with 300 μm thickness and the resulted film was submerged into distilled water at 25 °C following the initial phase separation and membrane solidification. Later on, the membrane was preserved in fresh distilled water for 24 h in

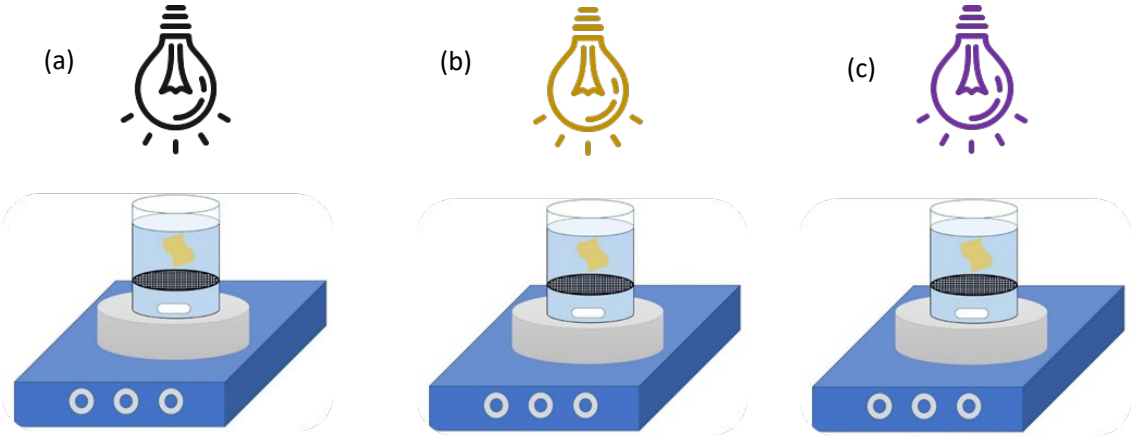

Fig. 1. Schematic representation of the photodegradation setup in (a) dark, (b) Visible light and (c) UV light ambient

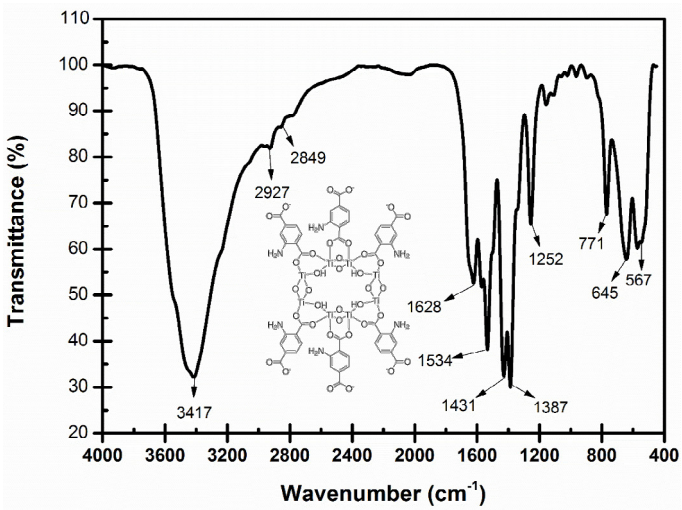

Fig. 2. FTIR spectra for NH_2-MIL125(Ti) MOF

order to ensure full phase inversion [30]. As the solvent is removed from the film layer, flat sheet polymeric membrane would be achieved.

Evaluation of photocatalytic activity

The photocatalytic performance of the fabricated membranes was investigated by measuring the degradation rate of Methylene Blue (MB) in darkness, visible light, and under UV irradiation. A strip (8 cm x 8 cm) of the polymeric membrane was suspended in 100 mL of MB solution (10 ppm) under the mentioned light conditions (Fig. 1). The UV irradiation was obtained from an ultraviolet (UVC) lamp (Philips Electronics, Poland, λ= 253.7 nm, 6 W). On the other hand, the visible light irradiation is obtained from white light-emitting diode (LED) floodlight (EDC, Iran, λ> 420 nm, 6 W).

Prior to the photocatalytic reactions, the solutions were stirred on a magnet stirrer in the dark environment for an hour in order to achieve adsorption/desorption equilibrium. 2mL aliquots of the dye solution, that is being treated, were withdrawn using a disposable syringe at 60 minutes intervals for 300 minutes. Variations in the concentration of MB under illumination were monitored using a UV-Vis spectrophotometer (2120UV PLUS, Optizen) at λ = 665nm.

RESULTS AND DISCUSSION

Characterization of NH_2-MIL125(Ti)

The chemical structure of NH_2-MIL125(Ti) was analyzed by FT-IR (Fig. 2). The spectra were characterized by high-intensity peaks in the region 4000 cm^{-1} to 400 cm^{-1}. Regarding the results of

Table 2. FTIR peak assignments

Peak Position (cm^{-1})	Peak Assignment
3417	tensile vibration of the O-H and N-H groups
2927	Asymmetric tensile vibrations of the C-H bands in the $-CH_2$ structure
2849	symmetric tensile vibrations of the C-H bands in the $-CH_2$ structure
1628	flexural vibration of N-H bonds
1534	carboxylate ligands
1431	carboxylate ligands
1387	oscillatory vibration of $-CH_2$ groups
1252	tensile vibration of C-N bonds at aromatic amines
800-400	O-Ti-O vibration

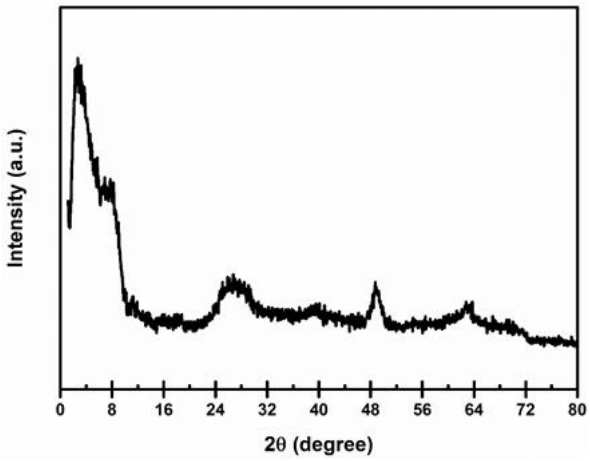

Fig. 3. XRD spectrum of the NH_2-MIL125(Ti)

the FTIR test, it could be concluded that NH_2-MIL125(Ti) is existing in the studied system.

Specific bands and their assignments are summarized in Table 2 [31-33].

The crystal structure of NH_2-MIL125 (Ti) was identified by XRD (Fig. 3). It could be observed that NH_2-MIL125(Ti) was mainly amorphous which is in agreement with FE-SEM observations and presented one prominent peak at 2θ =3° [30]. Peaks at low diffraction pattern angles, 2θ value of 3 and 10 degrees respectively corresponding to the (101) and (002) planes, and peaks at four prominent diffractions at 2θ= 20°, 28°, 48°, and 63°, confirm the formation of the NH_2-MIL125(Ti) phase in the structure [34]. This structure contains chains of μ-OH corner-sharing TiO_6 octahedral, which are interconnected by NH_2-BDC molecules in order to form three-dimensional pores [35].

Fig. 4 shows the results of investigation on the surface morphology of the NH_2-MIL125(Ti) by the FE-SEM test. According to the results, the surface of the sample (at 1000x magnification) includes a sheet of aggregated particles, which is more visible in part (c). Due to the surface-to-volume ratio of these nanoparticles and their high surface energy, they are clinging together and forming clusters in order to achieve a more stable state of the nanoparticles.

Characterization of NH_2-MIL125(Ti)/PSf membrane

The FE-SEM images of the NH_2-MIL125(Ti)/PSf membrane system containing different amounts (0, 0.2, 0.5, and 1%) of MOF are shown in Fig. 5. As shown in Fig. 5(a), no particle is visible in the pure PSf membrane sample and a large clean surface is obvious in the image. By applying MOF into the polymer matrix, the surface morphology of the nanocomposite changes, and particles of different dimensions could be observed on the surface of the samples. Regarding Fig. 5, by increasing the percentage of MOF in the nanocomposite, the number and the size of the particles, presenting on the polymer surface, have increased so that the average size of these particles became almost 32.4

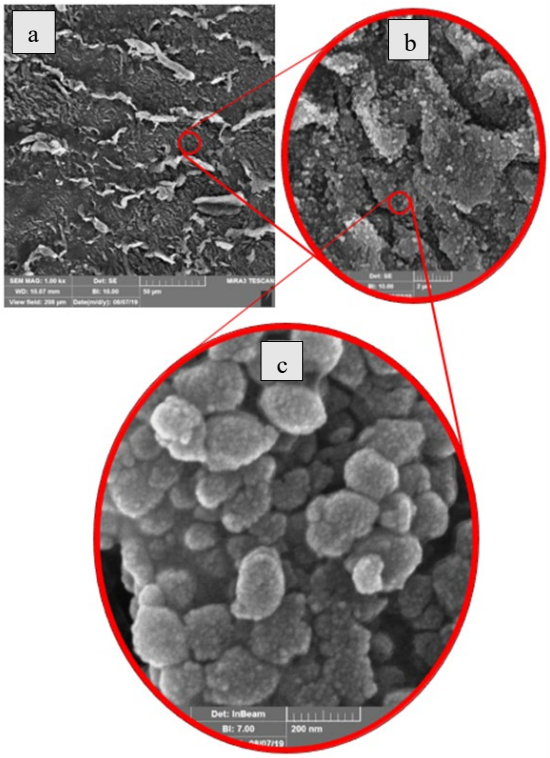

Fig. 4. FESEM images morphology of the NH_2-MIL125(Ti) surface investigated at three different magnifications (a) 1000, (b) 15000 and (c) 200000 times

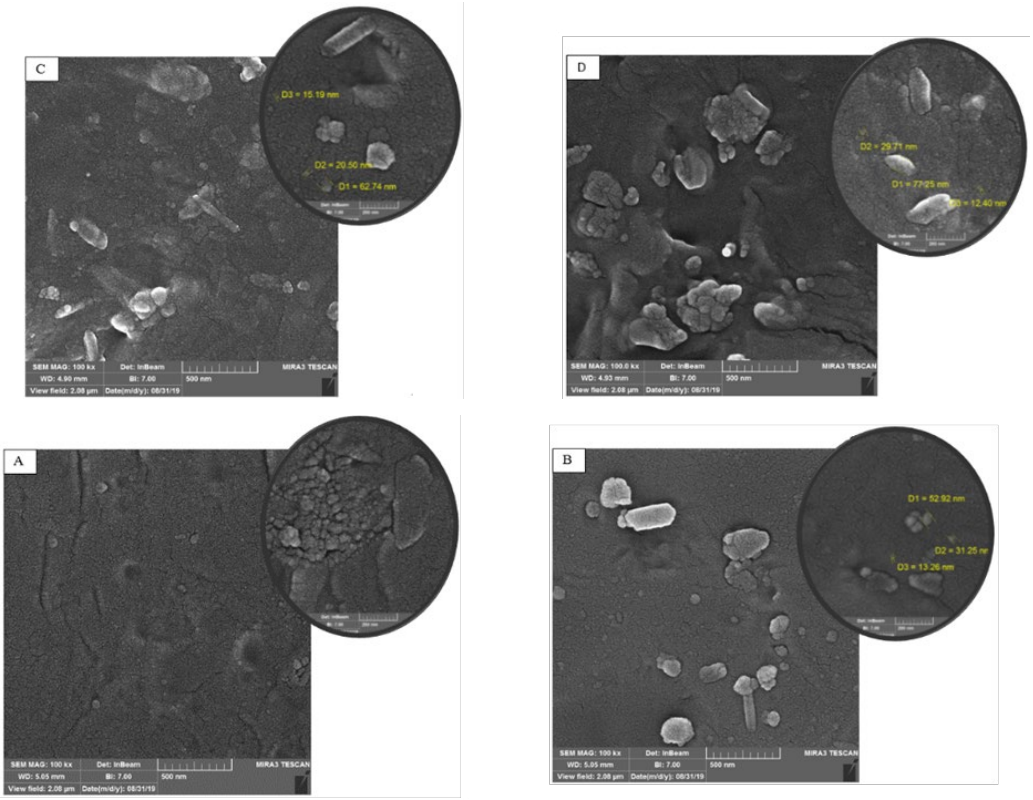

Fig. 5.A. (a) FESEM images of PSf membrane sample and PSf membrane sample containing (b) 0.2, (c) 0.5 and (d) 1% MOF

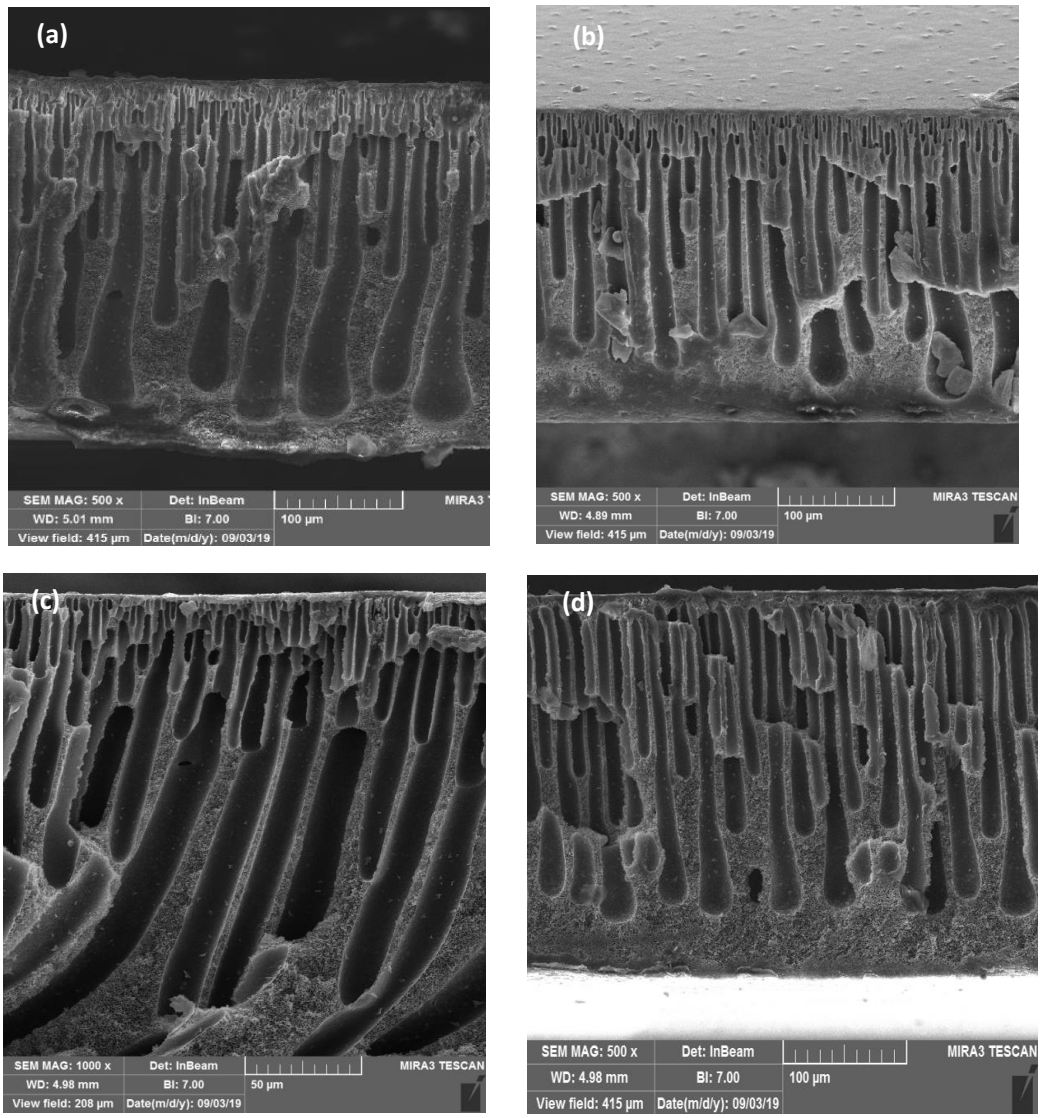

Fig. 5.B. SEM images from the cross-section morphology of NH_2-MIL125(Ti)/PSf membrane: a) PSf b) PSfM0.2 c) PSfM0.5 d) PSfM1

nm in the PSf sample. By increasing the composition of MOF in the PSf polymer matrix, the number and size of these particles have increased and reached a size of 38.8 nm. These results indicate that despite the increase in the percentage of MOF from 0.2 to 0.5 wt. %, no significant effects have been made on particle agglomeration, and the dispersal performance was respectably at 0.5 wt. %. However, by a further increase in the MOF percentage of the polysulfonate structure, particle scattering was affected and as the particles are agglomerating within the polymer matrix structure, they reach a growth rate of about 20%. This mode of clustering in the low magnified image is also evident in Fig. 5(d). Particle agglomeration could affect the final characteristics of the system and change some of the nanocomposites properties.

Fig. 5.B. shows the images from the cross-section of the NH_2-MIL125(Ti)/PSf membrane with different compositions. It could be observed that the density and quantity of the membrane pore have gradually enlarged by increasing the concentration of NH_2-MIL125(Ti) in the membrane. From this cross-section morphology, it could be observed that all membranes have a homogeneous porous internal structure. Moreover,

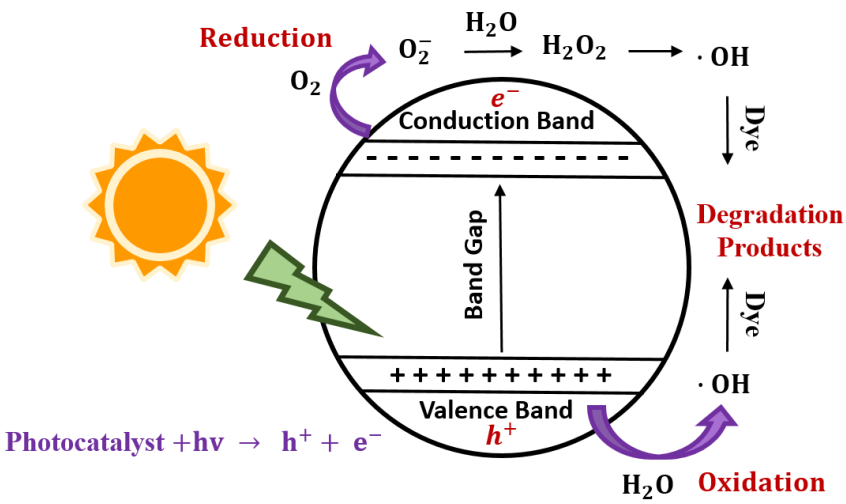

Fig. 6. Proposed mechanism for photocatalytic degradation of Methylene Blue dye over NH2-MIL125(Ti)/Polysulfone membrane under irradiation

the sponge-like bottom layer, intermediate layer, and top skin layer show a typical asymmetrical structure. On the other hand, the presence of NH_2-MIL125(Ti) in the membrane structure plays a significant role in hydrophilic characteristics and photocatalytic activity of the membrane surface.

The photocatalytic performance of NH_2-MIL125(Ti)

The details of the reactions and mechanisms of MOF in the PSf polymer matrix for MB's photocatalytic degradation are presented in Fig. 6. When MOF is exposed to visible and UV light irradiation with energy equal or greater than their band gaps, the electrons (e^-) are excited by photo-induced from the highest occupied molecular orbital (HOMO) (6.4 eV) to the lowest unoccupied molecular orbital (LUMO) (3.8 eV), thus leaving the holes (h^+) in the valence band. The excited electrons (e^-) might be directly entrapped by the molecular oxygen dissolved in solution in order to form superoxide radicals ($O_2^{-\bullet}$). The produced holes (h^+) are reacted with water molecules or hydroxyl ions (-OH) in order to produce hydroxyl radicals ($OH^\bullet$), which oxidize and degrade the dye molecules. In addition, the photo-induced holes (h^+) could directly oxidize the MB molecules as well. O_2 reduction and H_2O oxidation could generate $O_2^{-\bullet}$ and $OH^\bullet$ [36], [37]. The reactions at the surface of the photocatalyst initiating the degradation of MB dye could be expressed as follows:

$$PSfM + h\nu \rightarrow e^- (CB) + h^+ (VB) \quad (1)$$

$$O_2 + e^- (CB) \rightarrow O_2^{-\bullet} \quad (2)$$

$$H_2O + h^+ (VB) \rightarrow OH^\bullet + H^+ \quad (3)$$

$$O_2^{-\bullet} + H^+ \rightarrow HOO^\bullet \rightarrow OH^\bullet \quad (4)$$

$$\text{Methylene Blue} + OH^\bullet \rightarrow \text{degradation of the dye} \quad (5)$$

$$\text{Methylene Blue} + h^+ (VB) \rightarrow \text{oxidation products} \quad (6)$$

$$\text{Methylene Blue} + e^- (CB) \rightarrow \text{reduction products} \quad (7)$$

Photodegradation kinetics follow the Langmr-Hinshelwood (L-H) model (Fig. 7(c), 8(c), 9(c)) where monolayer adsorption takes place on the nanoparticles' surfaces [38]. The reaction rate depends on the concentration of the pollutant according to Eq. 8:

$$r = \frac{dC}{dt} = -\frac{kKC}{1+KC} \quad (8)$$

where r is the rate of the reaction, C is the dye concentration in the solution, t is time, k is the reaction constant and K is the adsorption equilibrium factor for the pollutant on the photocatalyst surface. Assuming KC to be negligible, the equation could then be simplified to Eq. 9:

$$ln\frac{C}{C_0} = \frac{dC}{dt} = -k_{app}t \quad (9)$$

where C_0 is the initial concentration of dye, C is the concentration at time t and k_{app} is the apparent reaction constant [39].

The photocatalytic activity of NH_2-MIL125(Ti) nanoparticles for MB dye removal, was investigated under visible light [40] (Fig. 7). The effects of different

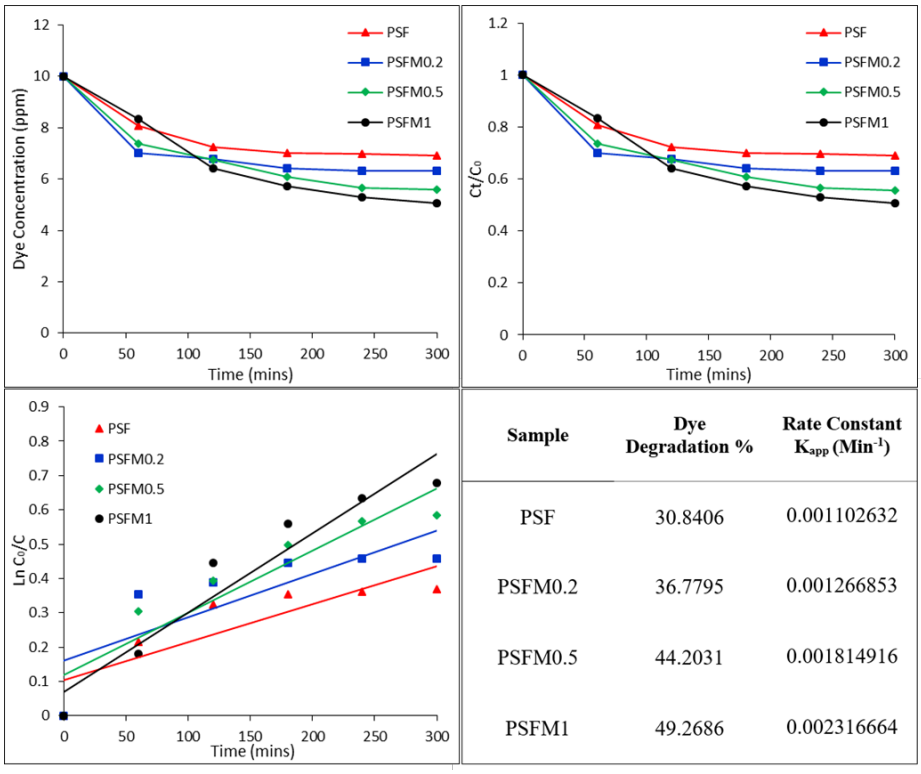

Sample	Dye Degradation %	Rate Constant K_{app} (Min^{-1})
PSF	30.8406	0.001102632
PSFM0.2	36.7795	0.001266853
PSFM0.5	44.2031	0.001814916
PSFM1	49.2686	0.002316664

Fig. 7. Photocatalytic activity of the membranes under Visible irradiation; (a) dye degradation, (b) normalized dye degradation, (c) degradation kinetics, (d) table of % degradation and rate constants

NH_2-MIL125(Ti)/PSf membrane compositions on Methylene Blue dye removal over 5 hours and under visible light is presented in Fig. 7. As shown in Fig. 7 (a,b), the percentages of dye removal for all PSfM samples are higher than the pure PSf membrane. PSfM1 shows the highest dye removal efficiency after 5 hours, and PSFM0.2 and PSfM0.5 became stable, respectively after 3 and 4 hours. According to Fig. 7(d), the rate constant of pure PSf membrane was lower (0.001102632 min^{-1}) than the loaded nanoparticle membranes, with PSFM1 showing the highest degradation rate (0.0023161664 min^{-1}). The results indicate that under visible light irradiation, adding excess amounts of NH_2-MIL125(Ti) nanoparticles causes severe agglomeration which decreases the active sites of the membrane [41].

Fig. 8 shows the effects of membrane composition on the removal of MB dye over 5 hours under UV irradiation. The rate constant of pure PSf membrane was lower than that of the nanoparticle loaded membranes, with PSfM1 showing the highest degradation rate (0.002757 min^{-1}) (Fig. 8(d)). MB dye would be adsorbed on the membrane surface and neutralizes the negative charges on the surface of the membrane. Also, under the UV light irradiation, the photocatalytic activity takes place inside the membrane which may lead to further degradation of MB. After a while, the adsorption sites of the membrane surface would be covered and the electrostatic adsorption forces between the membrane surface and MB becomes weaker which results in a decrease in the photocatalyst performance of the membrane [42].

Fig. 9 shows the removal of MB in the dark environment for 5 hours. In the dark environment experiment, the dye removal percentage was reduced down to 17% and 38% compared to the visible and UV irradiation, respectively. Fig. 9(a) shows that the removal of MB in the first 2 hours has an upgoing trend and afterward it becomes stable. In the dark environment, the rate constant of pure PSf membrane was lower (0.000957 min^{-1}) than that of the nanoparticle-loaded membranes, with PSFM1 showing the highest degradation rate (0.001337 min^{-1}) (Fig. 9(d)). In the dark environment, there are no photons in order to activate the electrons. It leads to the dominance of adsorption in the dye degradation process which results in an adsorption equilibrium [40]. According to Fig. 9 at the first 60 minutes of the adsorption process, dye molecules have a high

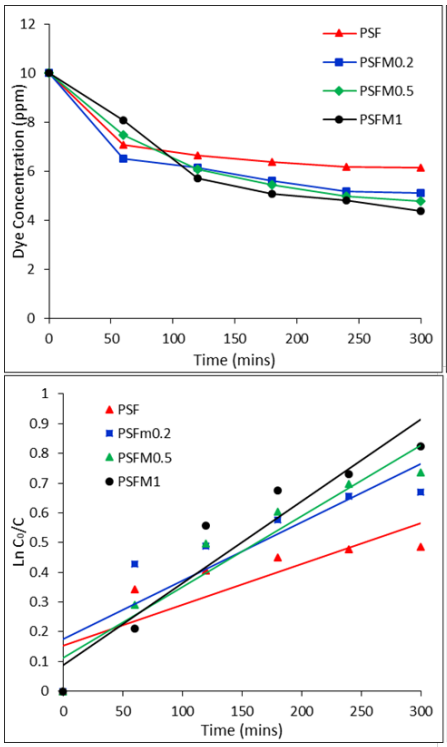

Sample	Dye Degradation %	Rate Constant K_{app} (Min^{-1})
PSF	38.5385	0.001374
PSFM0.2	48.8462	0.001962
PSFM0.5	52.0769	0.002386
PSFM1	56.0769	0.002757

Fig. 8. Photocatalytic activity of the membranes under UV irradiation; (a) dye degradation, (b) normalized dye degradation, (c) degradation kinetics, (d) table of % degradation and rate constants

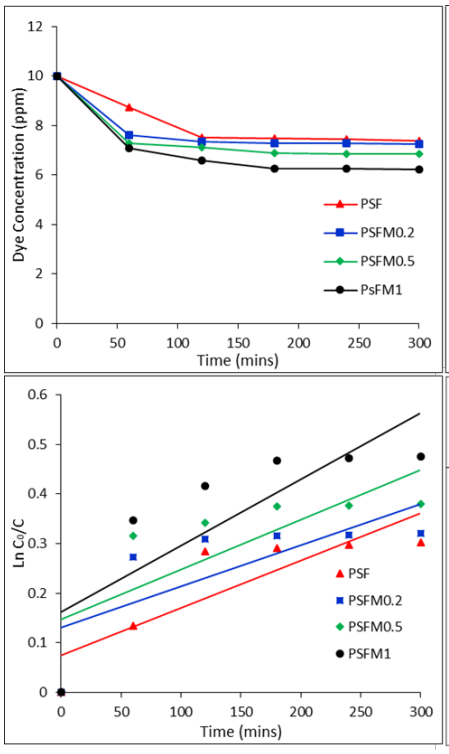

Sample	Dye Degradation %	Rate Constant K_{app} (Min^{-1})
PSF	26.1451	0.000957
PSFM0.2	27.3894	0.000829
PSFM0.5	31.5929	0.001007
PSFM1	37.8814	0.001337

Fig. 9. Photocatalytic activity of the membranes in the Dark environment; (a) dye degradation, (b) normalized dye degradation, (c) degradation kinetics, (d) table of % degradation and rate constants

tendency to be adsorbed onto the membrane's surface; however, after a while, this tendency would decrease and dye degradation rate gets almost stable [10].

From all of the above figures, it could be concluded that the entrapment by MOF, improved the photocatalytic performance of the PSf membranes. On the other hand, the results have showed that the reaction rate was low in the first hour and increased gradually overtime. This process could be explained by the hydrophilic properties of the membrane. As the physical and chemical modifications of the polymer are taking place, and polymer is being exposed to the absorption of electromagnetic radiation in the presence of oxygen molecules, short chains of d-sulfonic acid molecules would be released. Sulfonic acids are surfactants that significantly reduce the contact angle of the membrane and reduce the repulsion between the surface of the membrane and dye, resulting in the increase of dye penetration into the membrane [43].

CONCLUSIONS

The paper studied the phase inversion embedment of NH_2-MIL125(Ti) in PSf membranes for the photocatalytic removal of Methylene Blue from synthesized wastewater. The effects of NH_2-MIL125(Ti) dosage and various irradiations on membrane performance were investigated. The entrapment of NH_2-MIL125(Ti) into PSf membranes resulted in an enhancement of the membrane photoactivity, porosity, and hydrophilicity without compromising membrane integrity. Up to 60% of Methylene blue dye was removed after five hours of UV light irradiation of the membrane. By simple comparison, it was observed that there is a slight difference between the dye removal efficiency of being exposed to visible light on one hand and UV light irradiation on the other hand, which conducts us to prefer the visible light due to the availability of this irradiation source and not causing damage to the membrane structure. Unlike free photocatalytic nanoparticles, the membrane could easily be taken out of the system and be used again which significantly reduces the post-treatment costs. Studying the use of this membrane in the membrane system and its performance, are considered to be addressed in future work.

ACKNOWLEDGMENT

The authors gratefully acknowledge the assistance offered by the technical staff of UNESCO Chair on Water Reuse for conducting this research and also the Biotechnology Laboratory in the University of Tehran.

CONFLICT OF INTEREST

Author declares no conflict of interest.

REFERENCES

1. Fil BA, Ozmetin C, Korkmaz M. Cationic Dye (Methylene Blue) Removal from Aqueous Solution by Montmorillonite. Bulletin of the Korean Chemical Society. 2012;33(10):3184-90.
2. R Ananthashankar AEG. Production, Characterization and Treatment of Textile Effluents: A Critical Review. Journal of Chemical Engineering & Process Technology. 2013;05(01).
3. Berber-Villamar NK, Netzahuatl-Muñoz AR, Morales-Barrera L, Chávez-Camarillo GM, Flores-Ortiz CM, Cristiani-Urbina E. Corncob as an effective, eco-friendly, and economic biosorbent for removing the azo dye Direct Yellow 27 from aqueous solutions. PLOS ONE. 2018;13(4):e0196428.
4. Singh S, Sidhu GK, Singh H. Removal of methylene blue dye using activated carbon prepared from biowaste precursor. Indian Chemical Engineer. 2017:1-12.
5. Robinson, T., B. Chandran, and P. Nigam, *Removal of dyes from a synthetic textile dye effluent by biosorption on apple pomace and wheat straw.* Water research, 2002. **36**(11): p. 2824-2830.
6. Rafiee E, Pami N, Zinatizadeh AA, Eavani S. A new polyoxometalate-TiO2 nanocomposite for efficient visible photodegradation of dye from wastewater, liquorice and yeast extract: Photoelectrochemical, electrochemical, and physical investigations. Journal of Photochemistry and Photobiology A: Chemistry. 2020;386:112145.
7. Guimarães Gusmão KA, Alves Gurgel LV, Sacramento Melo TM, Gil LF. Application of succinylated sugarcane bagasse as adsorbent to remove methylene blue and gentian violet from aqueous solutions – Kinetic and equilibrium studies. Dyes and Pigments. 2012;92(3):967-74.
8. Habibi, A. and Z. Mehrabi, *Aerobic degradation of methylene blue from colored effluents by Ralstonia eutropha.* Pollution, 2017. **3**(3): p. 363-375.
9. Mahanthappa M, Kottam N, Yellappa S. Enhanced photocatalytic degradation of methylene blue dye using CuS CdS nanocomposite under visible light irradiation. Applied Surface Science. 2019;475:828-38.
10. Kausar A, Shahzad R, Iqbal J, Muhammad N, Ibrahim SM, Iqbal M. Development of new organic-inorganic, hybrid bionanocomposite from cellulose and clay for enhanced removal of Drimarine Yellow HF-3GL dye. International Journal of Biological Macromolecules. 2020;149:1059-71.
11. Samsami S, Mohamadi M, Sarrafzadeh M-H, Rene ER, Firoozbahr M. Recent advances in the treatment of dye-containing wastewater from textile industries: Overview and perspectives. Process Safety and Environmental Protection. 2020;143:138-63.
12. Zhang H, Quan X, Chen S, Zhao H, Zhao Y. Fabrication of photocatalytic membrane and evaluation its efficiency in removal of organic pollutants from water. Separation and Purification Technology. 2006;50(2):147-55.
13. Zheng X, Shen Z-P, Shi L, Cheng R, Yuan D-H. Photocatalytic Membrane Reactors (PMRs) in Water Treatment: Configurations and Influencing Factors. Catalysts. 2017;7(8):224.

14. Kumar S, Ahlawat W, Bhanjana G, Heydarifard S, Nazhad MM, Dilbaghi N. Nanotechnology-Based Water Treatment Strategies. Journal of Nanoscience and Nanotechnology. 2014;14(2):1838-58.
15. Zouhier M, Tanji K, Navio JA, Hidalgo MC, Jaramillo-Páez C, Kherbeche A. Preparation of ZnFe2O4/ZnO composite: Effect of operational parameters for photocatalytic degradation of dyes under UV and visible illumination. Journal of Photochemistry and Photobiology A: Chemistry. 2020;390:112305.
16. Benhabiles O, Galiano F, Marino T, Mahmoudi H, Lounici H, Figoli A. Preparation and Characterization of TiO2-PVDF/PMMA Blend Membranes Using an Alternative Non-Toxic Solvent for UF/MF and Photocatalytic Application. Molecules. 2019;24(4):724.
17. Zioui D, Salazar H, Audjit L, Martins P, Lanceros-Mendez S. Photocatalytic Polymeric Nanocomposite Membrane Towards Oily Wastewater. MDPI AG; 2019.
18. Kuvarega AT, Khumalo N, Dlamini D, Mamba BB. Polysulfone/N,Pd co-doped TiO2 composite membranes for photocatalytic dye degradation. Separation and Purification Technology. 2018;191:122-33.
19. Mohamed MA, W. Salleh WN, Jaafar J, Ismail AF, Mutalib MA, Sani NAA, et al. Physicochemical characteristic of regenerated cellulose/N-doped TiO 2 nanocomposite membrane fabricated from recycled newspaper with photocatalytic activity under UV and visible light irradiation. Chemical Engineering Journal. 2016;284:202-15.
20. Molinari R, Argurio P, Szymański K, Darowna D, Mozia S. Photocatalytic membrane reactors for wastewater treatment. Current Trends and Future Developments on (Bio-) Membranes: Elsevier; 2020. p. 83-116.
21. Ong CS, Lau WJ, Goh PS, Ng BC, Ismail AF, Choo CM. The impacts of various operating conditions on submerged membrane photocatalytic reactors (SMPR) for organic pollutant separation and degradation: a review. RSC Advances. 2015;5(118):97335-48.
22. Zhao X, Zhang Y, Wen P, Xu G, Ma D, Qiu P. NH2-MIL-125(Ti)/TiO2 composites as superior visible-light photocatalysts for selective oxidation of cyclohexane. Molecular Catalysis. 2018;452:175-83.
23. Fu Y, Sun D, Chen Y, Huang R, Ding Z, Fu X, et al. An Amine-Functionalized Titanium Metal-Organic Framework Photocatalyst with Visible-Light-Induced Activity for CO2 Reduction. Angewandte Chemie International Edition. 2012;51(14):3364-7.
24. Rezaei-DashtArzhandi M, Sarrafzadeh MH, Goh PS, Lau WJ, Ismail AF, Mohamed MA. Development of novel thin film nanocomposite forward osmosis membranes containing halloysite/graphitic carbon nitride nanoparticles towards enhanced desalination performance. Desalination. 2018;447:18-28.
25. Huang H-L, Yang S. Filtration characteristics of polysulfone membrane filters. Journal of Aerosol Science. 2006;37(10):1198-208.
26. Melvin Ng HK, Leo CP, Abdullah AZ. Selective removal of dyes by molecular imprinted TiO2 nanoparticles in polysulfone ultrafiltration membrane. Journal of Environmental Chemical Engineering. 2017;5(4):3991-8.
27. Jyothi MS, Nayak V, Padaki M, Geetha Balakrishna R, Soontarapa K. Aminated polysulfone/TiO2 composite membranes for an effective removal of Cr(VI). Chemical Engineering Journal. 2016;283:1494-505.
28. Nasalevich MA, Becker R, Ramos-Fernandez EV, Castellanos S, Veber SL, Fedin MV, et al. Co@NH2-MIL-125(Ti): cobaloxime-derived metal–organic framework-based composite for light-driven H2 production. Energy & Environmental Science. 2015;8(1):364-75.
29. Lalia BS, Kochkodan V, Hashaikeh R, Hilal N. A review on membrane fabrication: Structure, properties and performance relationship. Desalination. 2013;326:77-95.
30. Zinadini S, Rostami S, Vatanpour V, Jalilian E. Preparation of antibiofouling polyethersulfone mixed matrix NF membrane using photocatalytic activity of ZnO/MWCNTs nanocomposite. Journal of Membrane Science. 2017;529:133-41.
31. Ding Y, Liu F, Jiang Q, Du B, Sun H. 12-Hydrothermal Synthesis and Characterization of Fe3O4 Nanorods. Journal of Inorganic and Organometallic Polymers and Materials. 2012;23(2):379-84.
32. Oveisi M, Asli MA, Mahmoodi NM. MIL-Ti metal-organic frameworks (MOFs) nanomaterials as superior adsorbents: Synthesis and ultrasound-aided dye adsorption from multicomponent wastewater systems. Journal of Hazardous Materials. 2018;347:123-40.
33. Larkin, P., *Infrared and Raman spectroscopy: principles and spectral interpretation*. 2017: Elsevier.
34. Bobb JA, Ibrahim AA, El-Shall MS. Laser Synthesis of Carbonaceous TiO2 from Metal–Organic Frameworks: Optimum Support for Pd Nanoparticles for C–C Cross-Coupling Reactions. ACS Applied Nano Materials. 2018;1(9):4852-62.
35. Hu S, Liu M, Li K, Zuo Y, Zhang A, Song C, et al. Solvothermal synthesis of NH2-MIL-125(Ti) from circular plate to octahedron. CrystEngComm. 2014;16(41):9645-50.
36. Li X, Pi Y, Hou Q, Yu H, Li Z, Li Y, et al. Amorphous TiO2@NH2-MIL-125(Ti) homologous MOF-encapsulated heterostructures with enhanced photocatalytic activity. Chemical Communications. 2018;54(15):1917-20.
37. Wang H, Cui P-H, Shi J-X, Tan J-Y, Zhang J-Y, Zhang N, et al. Controllable self-assembly of CdS@NH2-MIL-125(Ti) heterostructure with enhanced photodegradation efficiency for organic pollutants through synergistic effect. Materials Science in Semiconductor Processing. 2019;97:91-100.
38. Kuvarega AT, Krause RWM, Mamba BB. Nitrogen/Palladium-Codoped TiO2 for Efficient Visible Light Photocatalytic Dye Degradation. The Journal of Physical Chemistry C. 2011;115(45):22110-20.
39. Cobb, J.E. and R.L. Byberg, *Photocatalytic degradation of a series of direct azo dyes using immobilized TiO2*. 2012.
40. Huang L, Liu B. Synthesis of a novel and stable reduced graphene oxide/MOF hybrid nanocomposite and photocatalytic performance for the degradation of dyes. RSC Advances. 2016;6(22):17873-9.
41. Wang Q, Yang C, Zhang G, Hu L, Wang P. Photocatalytic Fe-doped TiO2/PSF composite UF membranes: Characterization and performance on BPA removal under visible-light irradiation. Chemical Engineering Journal. 2017;319:39-47.
42. Pereira VR, Isloor AM, Bhat UK, Ismail AF, Obaid A, Fun H-K. Preparation and performance studies of polysulfone-sulfated nano-titania (S-TiO2) nanofiltration membranes for dye removal. RSC Advances. 2015;5(66):53874-85.
43. Bormashenko E, Pogreb R, Whyman G, Bormashenko Y, Jager R, Stein T, et al. The Reversible Giant Change in the Contact Angle on the Polysulfone and Polyethersulfone Films Exposed to UV Irradiation. Langmuir. 2008;24(12):5977-80.